PNAS
www.pnas.org

Supplementary Information for

Slow expanders invade by forming dented fronts in microbial colonies

Hyunseok Lee, Jeff Gore, Kirill S. Korolev

Kirill S. Korolev.
E-mail: korolev@bu.edu

This PDF file includes:

Supplementary text
Figs. S1 to S13 (not allowed for Brief Reports)
SI References

Supporting Information Text

Contents

Supplementary figures

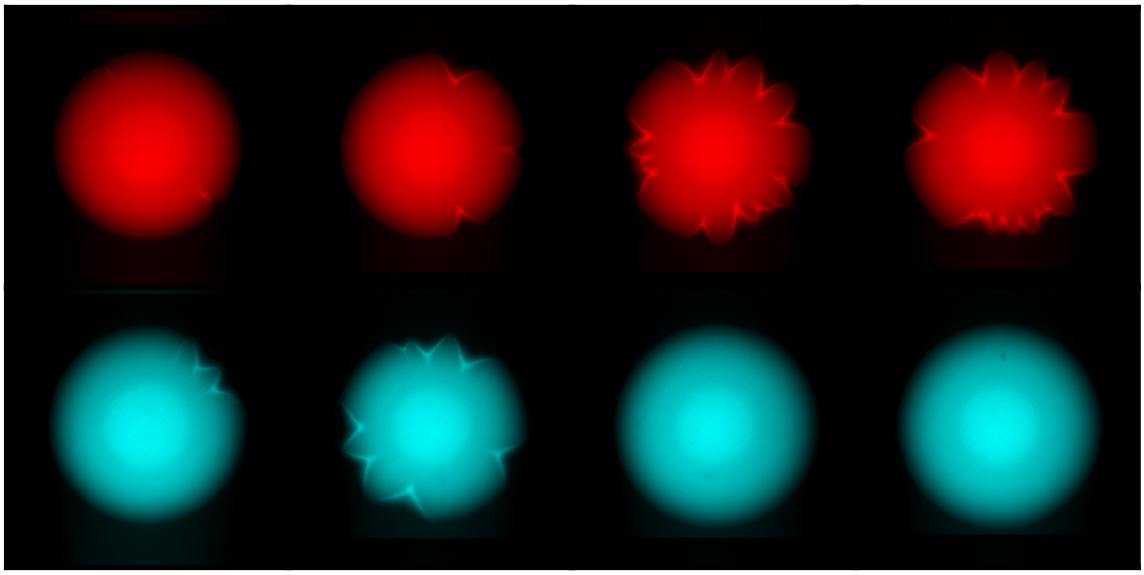

Fig. S1. Emergence of dents in wildtype colonies was reproducible. Wildtype colonies were grown for 48 hours. Top: wildtype strains constitutively expressing mScarlet-I. Bottom: wildtype strains constitutively expressing mTurquois-2.

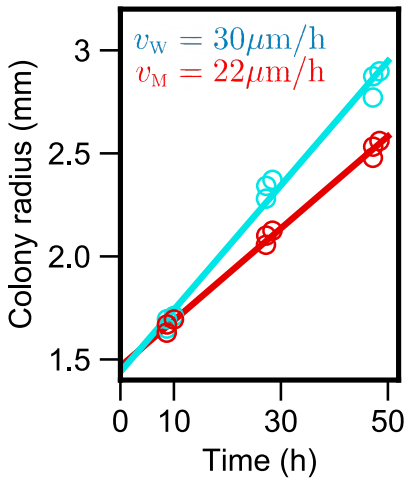

Fig. S2. Mutant expands more slowly regardless of the choice of fluorescent labels. Wildtype with mTurquoise-2 fluorescence protein expanded with $v_W = 30\ \mu m/h$ while mutant with mScarlet-I fluorescence protein expanded with $v_M = 22\ \mu m/h$.

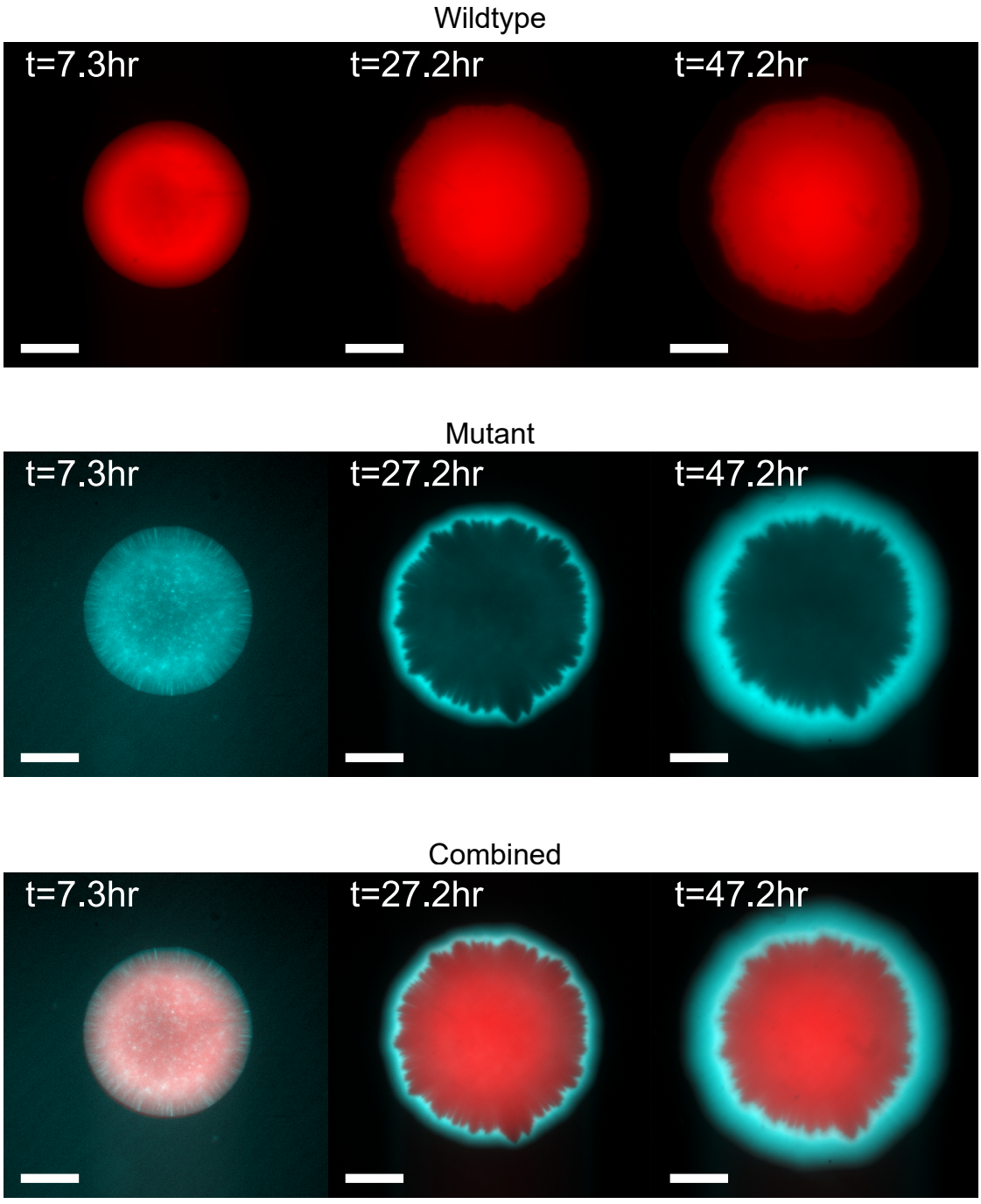

Fig. S3. In co-culture experiment, wildtype did not expand after a day while mutant kept expanding. Top: Fluorescence images of wildtype cells during expansion. Middle: Fluorescence images of mutant cells during expansion. Bottom: combined.

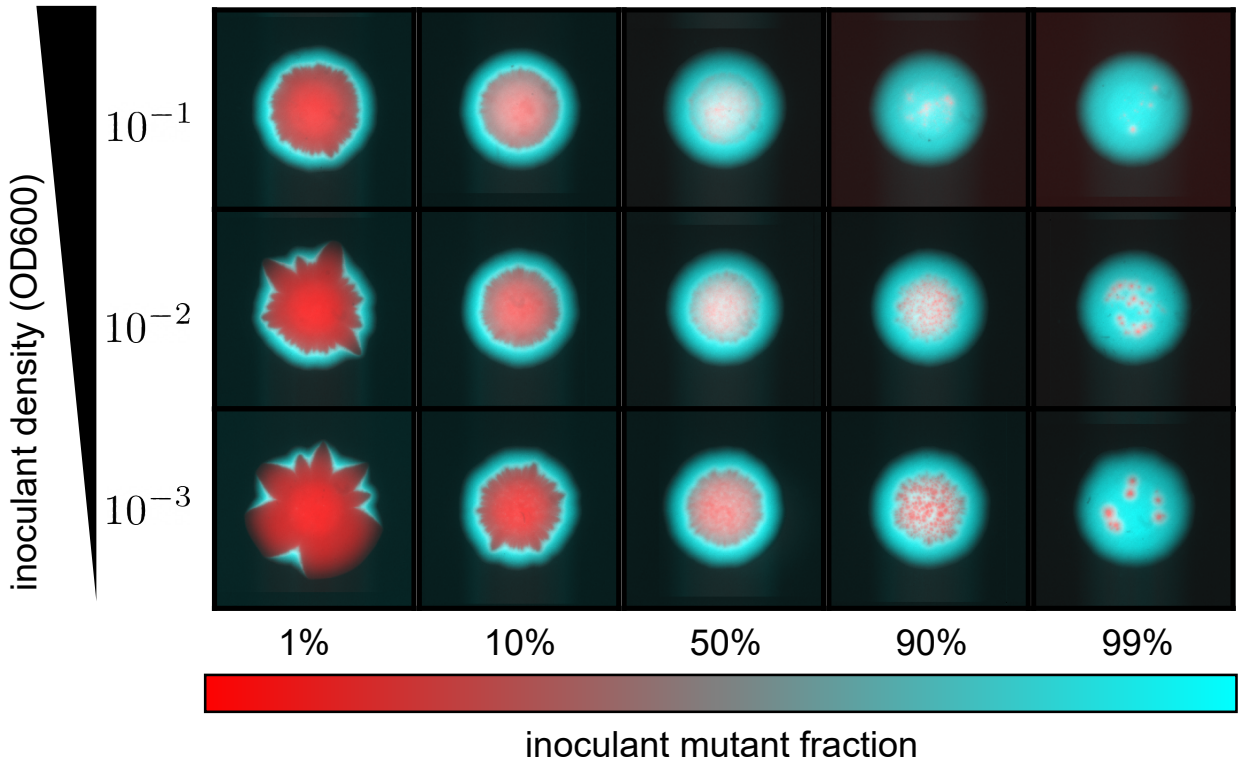

Fig. S4. Mutant outcompetes wildtype under a wide range of inoculant densities and initial mutant fractions.

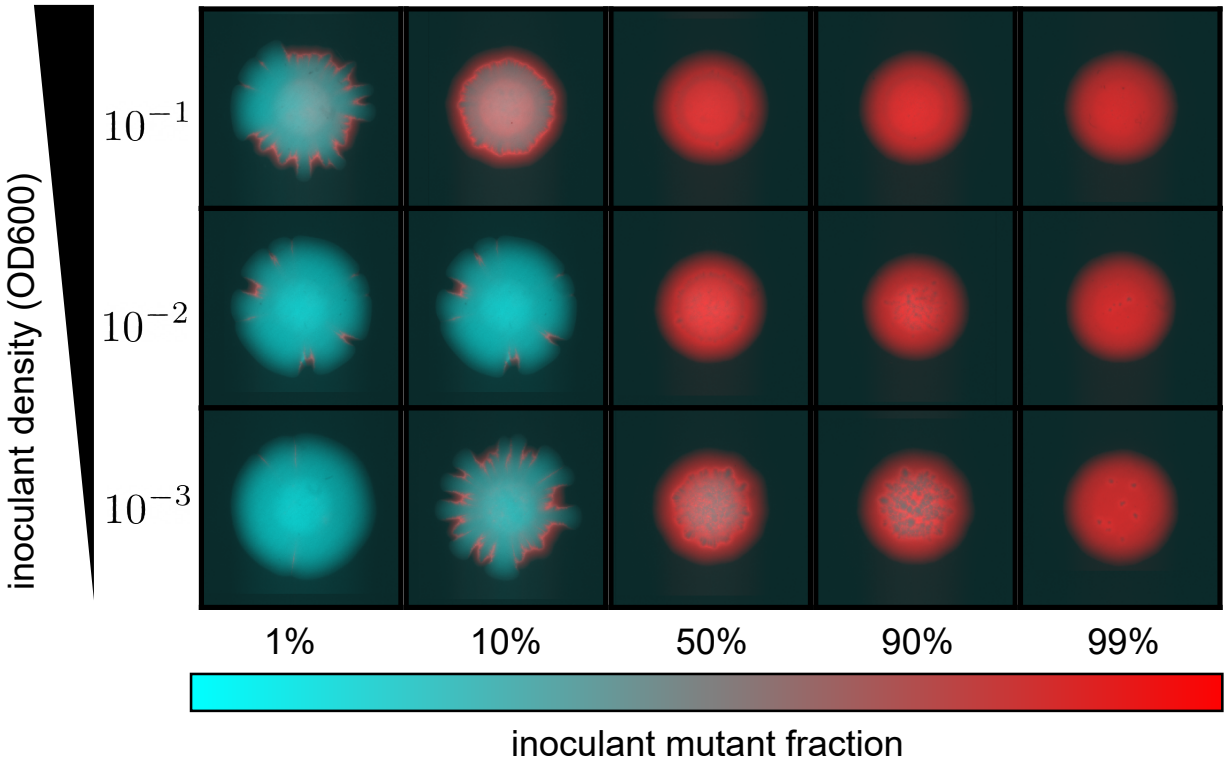

Fig. S5. Mutant outcompetes wildtype under a different choice of fluorescent labels of wildtype and mutant.

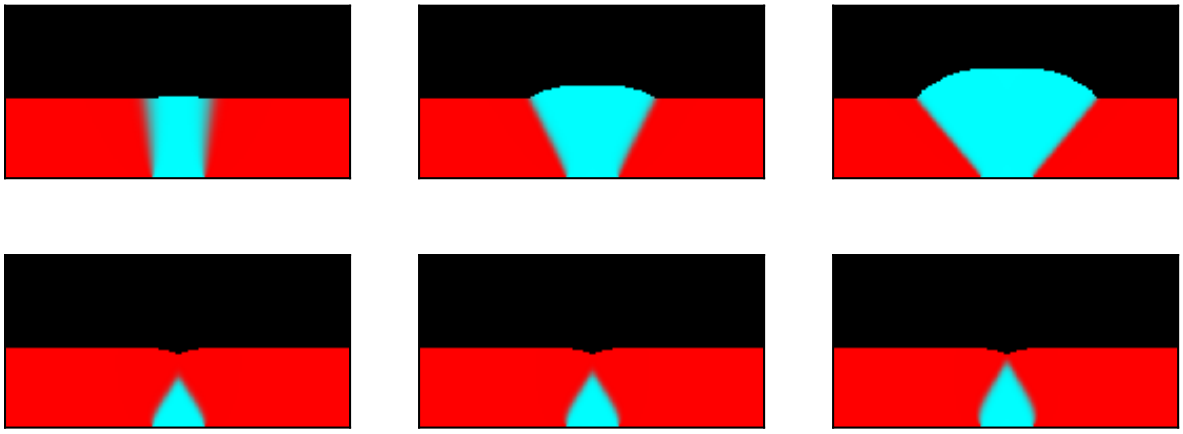

Fig. S6. No dented fronts occur in simulations with density-independent growth and dispersal. In each column, the growth advantage $r_{\mathsf{M}}/r_{\mathsf{W}} - 1$ is the same (Left: 0.04, Middle: 0.36, Right:1). Simulations in top row have $D_{\mathsf{W}} = D_{\mathsf{M}}$, so that the ratio of the expansion velocities varies with the growth rates ($v_{\mathsf{M}} = v_{\mathsf{W}}\sqrt{r_{\mathsf{M}}/r_{\mathsf{W}}}$). For the bottom row, we used $D_{\mathsf{M}} = \frac{0.64 r_{\mathsf{W}}}{r_{\mathsf{M}}} D_{\mathsf{W}}$ so that $v_{\mathsf{M}} = 0.8 v_{\mathsf{W}}$. We observed no expanding mutant sectors when its expansion velocity was less than that of the wildtype.

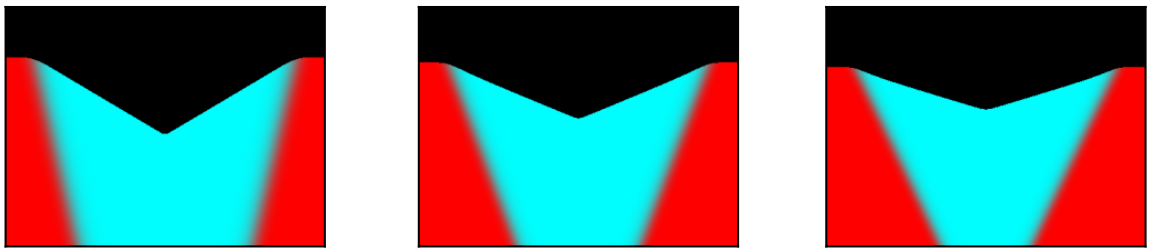

Fig. S7. Dented fronts occur in simulations with $D_{\mathrm{M}} \neq D_{\mathrm{W}}$. We used a variation of cheater-cooperator model (Eq. 2) in which dispersal of wildtype and mutant is no longer identical. In all cases of $D_{\mathrm{M}} = 0.9D_{\mathrm{W}}$, $D_{\mathrm{M}} = D_{\mathrm{W}}$, and $D_{\mathrm{M}} = 1.1D_{\mathrm{W}}$ mutant developed a dented front with only quantitative changes in sector shapes. These simulations used parameters $s = 0.4$ and $\alpha = 0.6$.

1. Geometric theory and sector shapes

A. Introduction. During spatial growth in microbial colonies or other cellular aggregates, mutants appear and compete with each other. Previous studies (1) and common intuition suggest that advantageous mutants should form a sector that bulges out of the expansion front. In the main text, we reported experiments showing that this is not always the case. Here, we identify all possible shapes that can result from competition between two types in a growing colony.

To make progress, we make a number of approximations and work in the so-called geometrical optics limit. This limit assumes that the expansion front and the boundary between the types can be treated as thin lines. Neglecting sector and boundary widths is justified when these length scales are much smaller than the colony size. In small colonies, thin boundaries require strong genetic drift and slow motility. Furthermore, we assume that the expansion velocity of each type remains fixed. In particular, we neglect the effects of spatial variation in nutrient concentration due to protrusions of one type ahead of the other. This approximation is valid for high nutrient concentrations and when the size of the protrusions is small compared to the size of the mutant sector.

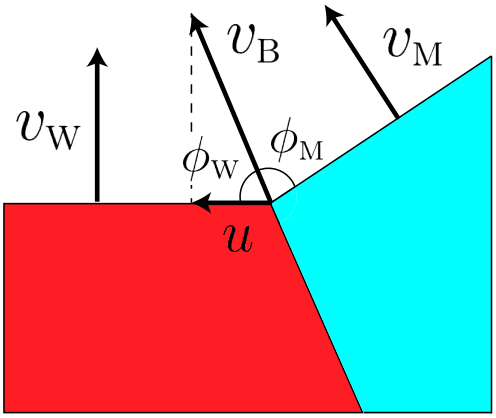

Fig. S8. Geometry of the competition.

In the geometric-optics limit, the competition between two types is described by three velocities: the velocity of mutant v_M, the velocity of wildtype v_W, and the velocity of the boundary v_B, which are shown in Fig. S8. (Note $v_B \neq u$) Previous work (1) focused on the regime when v_B was determined by v_M and v_W; in contrast, we make no assumptions about the relative magnitude of these three velocities.

To avoid confusion we want to reiterate that the velocity of the wildtype v_W is defined in isolation, away from the mutant. Similarly, the velocity of the mutant v_M is defined in isolation, away from the wildtype. For brevity, we refer to wildtype as fast and mutant as slow even though this terminology is not applicable at the sector boundary where the mutant may expand faster than the wildtype.

In the close vicinity of the sector boundary, the two expansion fronts can be approximated as straight lines. Their position (Fig. S8) is determined by requiring that the expansion along the boundary with velocity v_B results in the same displacement of the fronts as moving perpendicular to them with velocities v_M and v_W respectively:

$$v_W = v_B \sin \phi_W, \quad [1]$$

$$v_M = v_B \sin \phi_M. \quad [2]$$

For linear inoculations, the above equations are sufficient to completely specify sector shapes because, as we show below, the expansion fronts are straight lines even away from the sector boundary. For circular initial conditions, Eqs. (2) provide information only about the local orientation at the sector boundary, and further calculations are necessary. One way to obtain global shape is to write down partial differential equations that specify how the position of the front changes and use Eqs. (2) as the boundary conditions. A much simpler approach is to use an equal time argument from Ref. (1).

This method traces the ancestral lineage from each point along the front and requires that the time traveled on that lineage is equal to the current time t. The location of the ancestral lineage is such that it takes the shortest time to reach the initial population starting from a given point without entering the space occupied by the other type. The details of these calculations are provided below.

Before proceeding, we note that, here and in the main text, we typically parameterize the problem with velocity u rather than v_B. Since u is defined as the velocity of the boundary point along the front of wildtype, we can obtain it by projecting the boundary velocity on the expansion front of the wildtype:

$$u = v_B \cos \phi_W. \quad [3]$$

From this equation and Eq. (2), it follows that

$$v_{\text{B}} = \sqrt{v_{\text{W}}^2 + u^2}. \quad [4]$$

In the following, we assume that mutant takes over the front, i.e. $u > 0$. Mutants with negative u immediately become extinct at least in the deterministic model considered here.

Finally, we observe that Eqs. (2) impose constraints on the values of the three velocities. In particular, since sines are always less than one, the boundary velocity v_{B} must be greater or equal than both v_{M} and v_{W}. In terms of u, this implies that

$$v_{\text{M}} \leq \sqrt{u^2 + v_{\text{W}}^2}. \quad [5]$$

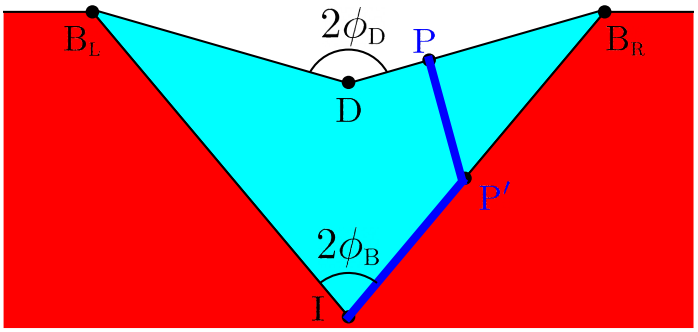

Fig. S9. Sector shape for linear inoculation and $v_{\text{M}} < v_{\text{W}}$. Sectors of faster wildtype (red) and slower mutant (cyan) meet at sector boundary $\overline{IB}_{\text{L}}$ and $\overline{IB}_{\text{R}}$. It takes the shortest time for the mutant to go from its initial location at I to a point on the front P by first following $\overline{IP'}$ and then $\overline{P'P}$ (blue path). The resulting geometry can be characterized by two opening angles: $2\phi_{\text{B}}$ for the sector boundary and $2\phi_{\text{D}}$ for the expansion front.

B. Linear inoculation.

B.1. Sector boundary. Linear expansion geometry, the simplest situation to consider, allows us to explain the essence of the equal time argument. This geometry is illustrated in Fig. S9. Initially ($t = 0$), the colony front is located at $y = 0$, and expansion proceeds in the upper half-plane. Mutant is only present at a single point, which we put at $x = 0$; the rest of the front is occupied by the wildtype.

As the expansion proceeds, the region near $x = 0$ is affected by the competition between the types. From the definition of u, the extent of this region is given by $x \in (-ut, ut)$. Regions further away are however unaffected and expand as if only wildtype is present. Thus, for $|x| \geq ut$, the front is located at $y = v_{\text{W}}t$. From these considerations, we can further conclude that the sector boundary is described by $(ut, v_{\text{W}}t)$. Note that, below, we consider only the right side of the expansion; the left side is described by the mirror image with respect to the y-axis. Thus,

$$\tan\phi_{\text{B}} = \frac{u}{v_{\text{W}}}. \quad [6]$$

Note that, $\phi_{\text{B}} = \phi_{\text{W}} - \pi/2$, which is clear from Figs. S8 and S9.

The shape of the front for $|x| < ut$ depends on the relative values of v_{M}, v_{W}, and u.

B.2. $v_{\text{M}} \leq v_{\text{W}}$**.** When mutant is slower than wildtype, we find that front has a V-shaped dent with an opening angle $2\phi_{\text{D}}$ as shown in Fig. S9. To derive this result, we take a point P on the front with yet unknown coordinates (x_p, y_p). Note that $x_p \in (0, ut)$. Then, we should obtain the location of the ancestral lineage that connects this point to the initial location of the mutant: point I. Because the ancestral lineage is located so that to minimize the travel time, it must be a union of straight lines. Indeed, it is a well-known fact from geometrical optics that light rays travel on straight lines except where the value of the refraction index changes (2). In our case, this means that the ancestral lineages of mutant can consist of straight lines within the mutant sector and regions of the boundary. Obviously, the ancestral lineage of the mutant cannot penetrate the region occupied by the wildtype.

The equal time argument then offers us two possibilities: a direct connection $\overline{IP}$ and an indirect connection $I\overset{\frown}{P'P}$ via a point P' on the sector boundary. The times to traverse these paths are

$$T_{PI} = |PI|/v_{\text{M}}, \quad [7]$$
$$T_{PP'I} = |PP'|/v_{\text{M}} + |P'I|/v_{\text{B}}. \quad [8]$$

To complete the analysis, we need to choose the path with the lowest travel time and determine all locations of P for which the travel time equals t. For the direct connection, it is clear that P must lie on an arc of a circle with the radius of $v_{\text{M}}t$ centered at I. For the indirect connection, we first need to determine the location of P', which must minimize the travel time.

Since P' lies on the sector boundary its coordinates are given by $(ut', v_{\text{W}}t')$ with an unknown t'. The travel time is then given by

$$T_{PP'I} = \frac{\sqrt{(x_p - ut')^2 + (y_p - v_{\text{W}}t')^2}}{v_{\text{M}}} + \frac{\sqrt{u^2 + v_{\text{W}}^2}t'}{v_b}. \quad [9]$$

Upon minimizing $T_{PP'I}$ with respect to t', we find that

$$t' = \frac{u\sqrt{u^2 + v_{\text{W}}^2 - v_{\text{M}}^2} + v_{\text{M}}v_{\text{W}}}{(u^2 + v_{\text{W}}^2)\sqrt{u^2 + v_{\text{W}}^2 - v_{\text{M}}^2}} \left(x_p + \frac{uv_{\text{W}} - v_{\text{M}}\sqrt{u^2 + v_{\text{W}}^2 - v_{\text{M}}^2}}{u^2 - v_{\text{M}}^2} y_p \right), \quad [10]$$

and the travel time equals

$$T_{PP'I} = \frac{(uv_{\text{M}} - v_{\text{W}}\sqrt{u^2 + v_{\text{W}}^2 - v_{\text{M}}^2})x_p + (v_{\text{M}}v_{\text{W}} + u\sqrt{u^2 + v_{\text{W}}^2 - v_{\text{M}}^2})y_p}{(u^2 + v_{\text{W}}^2)v_{\text{M}}}, \quad [11]$$

which is smaller than T_{PI} as long as $v_{\text{M}} < v_{\text{W}}$. Thus, the ancestral lineages takes an indirect path that first connects point P to the sector boundary and then follows the sector boundary until I. The shape of the front is determined by setting $T_{PP'I}$ from Eq. (11) equal to t. This results in a segment of a straight line, and a straightforward calculation shows that

$$\phi_{\text{D}} = \arctan\left(\frac{u\sqrt{v_{\text{W}}^2 + u^2 - v_{\text{M}}^2} + v_{\text{M}}v_{\text{W}}}{v_{\text{W}}\sqrt{v_{\text{W}}^2 + u^2 - v_{\text{M}}^2} - uv_{\text{M}}} \right). \quad [12]$$

Because the front and the sector boundaries are straight, the result above also directly follows from Eqs. (S8). Indeed, a simple geometric argument shows that $\phi_{\text{D}} = \phi_{\text{M}} + \phi_{\text{W}} - \pi/2$.

Note that, for $v_{\text{M}} = v_{\text{W}}$, the angle $\phi_{\text{D}} = \pi/2$ and the whole front is flat as it should if the expansion rates of the strains are identical.

B.3. $v_{\text{M}} = \sqrt{v_{\text{W}}^2 + u^2}$**.** In the limiting case of maximal allowed v_{M}, the shape of the sector is also simple and immediately follows from the calculations above. Now, as we compare the two alternative paths, we find that T_{PI} is always smaller than $T_{PP'I}$. Thus, the shape of the sector is an arc of a circle of radius $v_{\text{M}}t$ around I that connects to the flat front of the wild type at the sector boundary.

Previous work that used the equal time argument to describe competition in microbial colonies only considered $v_{\text{M}} = \sqrt{v_{\text{W}}^2 + u^2}$ and missed other possible front shapes (1). While it might appear that $v_{\text{M}} = \sqrt{v_{\text{W}}^2 + u^2}$ is a very special case, this relationship between the velocities holds across a wide set of conditions. Specifically, $v_{\text{M}} = \sqrt{v_{\text{W}}^2 + u^2}$ whenever local competition between the types is not strong enough to alter the priority effects due to different expansion velocities.

B.4. $v_{\text{W}} < v_{\text{M}} < \sqrt{v_{\text{W}}^2 + u^2}$**.** The remaining possibility is the hybrid of the two cases considered so far. Depending on how far P is from the sector boundary, the quickest path from P to I may be either the direct or the indirect connection. We find that the front around $x = 0$ is a semicircle of radius $v_{\text{M}}t$, but it is a straight line near the sector boundaries. The two segments joint smoothly. The angular half-width of the central arc, $\phi_{\text{transition}}$, and the slope of the linear segment (see Fig. S10) are given by

$$\phi_{\text{transition}} = \arctan\left(\frac{uv_{\text{M}} - v_{\text{W}}\sqrt{v_{\text{W}}^2 + u^2 - v_{\text{M}}^2}}{v_{\text{M}}v_{\text{W}} + u\sqrt{v_{\text{W}}^2 + u^2 - v_{\text{M}}^2}} \right), \quad [13]$$

$$\text{slope} = -\frac{uv_{\text{M}} - v_{\text{W}}\sqrt{v_{\text{W}}^2 + u^2 - v_{\text{M}}^2}}{v_{\text{M}}v_{\text{W}} + u\sqrt{v_{\text{W}}^2 + u^2 - v_{\text{M}}^2}}. \quad [14]$$

C. Circular inoculation. We assume that the expansion starts at $t = 0$ when wildtype colony fills the circle with radius $r \le r_0$, and the mutant is present only at $I = (r_0, 0)$ in polar coordinates.

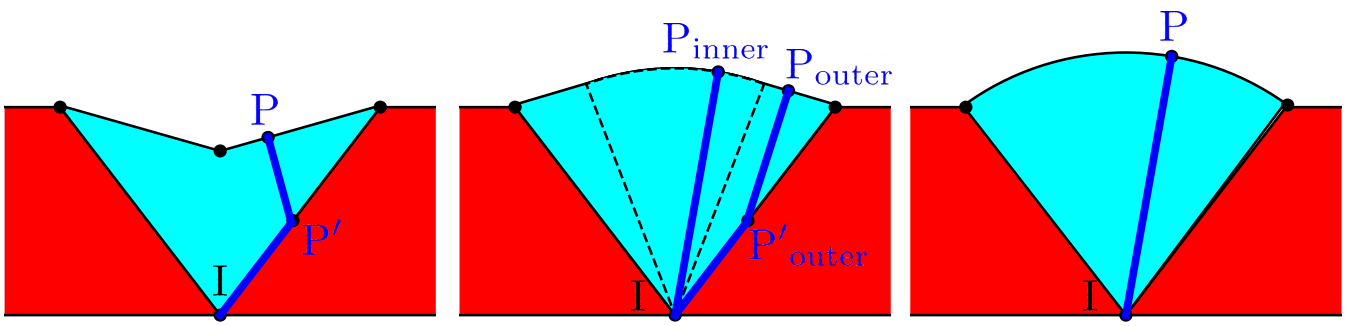

Fig. S10. Possible sector shapes for linear inoculation. Left: $v_{\text{M}} < v_{\text{W}}$. The mutant sector emerging from point I has a dented front. The front consists of two straight lines. The shortest-time path follows the sector boundary and also enters the sector interior. Middle: $v_{\text{W}} < v_{\text{M}} < \sqrt{v_{\text{W}}^2 + u^2}$. The mutant sector is a composite bulge. The front consists of two straight lines and an arc. To reach a point P_{outer} on straight part of the expansion front, the shortest-time path first follows the sector boundary before entering the sector interior. To reach a point P_{inner} on the arc, the shortest-time path follows a straight line from I to P_{inner}. Right: $v_{\text{M}} > \sqrt{v_{\text{W}}^2 + u^2}$. The front is an arc. To reach a point P on the front, the shortest-time path follows a straight line from I to P.

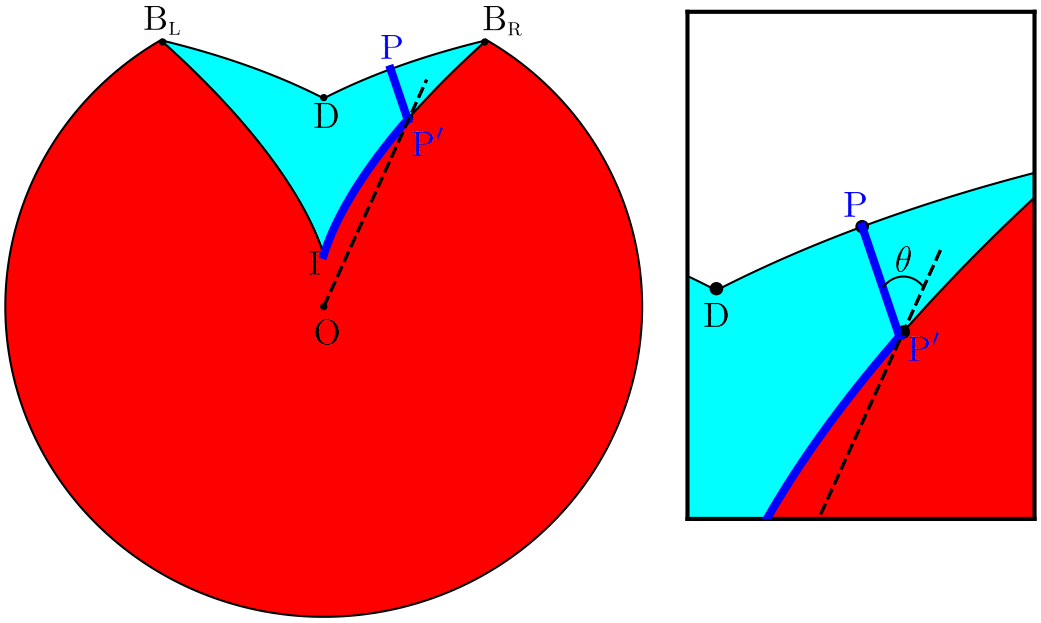

Fig. S11. Circular colony with a dented front, $v_{\text{W}} > v_{\text{M}}$. The path of the shortest time follows the sector boundary from I to P' and then a straight line connecting P' and P. Note that $\overline{P'P}$ and $\overline{OP'}$ always intersect at angle θ.

C.1. Sector boundary. The boundary between the mutant and the wild type moves with linear velocity u along the front.In polar coordinates, the position of the sector boundary $(r_{\text{B}}, \phi_{\text{B}})$ then obeys the following equation

$$\frac{d\phi_{\text{B}}}{dt} = \frac{u}{r_{\text{B}}}. \qquad [15]$$

We can eliminate time by using $dr_{\text{B}}/dt = v_{\text{W}}$ to obtain

$$\phi_{\text{B}}(r_{\text{B}}) = \frac{u}{v_{\text{W}}} \ln(\frac{r_{\text{B}}}{r_0}). \qquad [16]$$

We also find that the length of boundary at time t is $\sqrt{v_{\rm W}^2+u^2}t$, and thus

$$v_{\rm B}=\sqrt{v_{\rm W}^2+u^2} \tag{17}$$

just as in the linear case.

C.2. $v_{\rm M}<v_{\rm W}$. Let us consider a point $P=(r_p,\phi_p)$ on a mutant patch with $\phi_p>0$ for simplicity.

As described before, we first find $T_{PP'I}$ by minimizing $\frac{|PP'|}{v_{\rm M}}+\frac{|\overset{\frown}{P'I}|}{v_{\rm W}}$ over points P' on the sector boundary. The point $P'=(r_{P'},\phi_{P'})$ should satisfy two equations:

$$\phi_{P'}(r_{P'})=\frac{u}{v_{\rm W}}\ln(\frac{r_{P'}}{r_0}), \tag{18}$$

$$\frac{d}{dr_{P'}}\left(\frac{r_{P'}-r_0}{v_{\rm W}}+\frac{\sqrt{(r_p\cos\phi_p-r_{P'}\cos\phi_{P'})^2+(r_p\sin\phi_{P'}-r_{P'}\sin\phi_{P'})^2}}{v_{\rm M}}\right)=0. \tag{19}$$

Here, the first equation constrains P' to be on the sector boundary, and the second equation minimizes $T_{PP'I}$ over P'. Since there are two unknowns and two equations, we can solve for $(r_{P'},\phi_{P'})$. The solution is conveniently written in an implicit form:

$$\begin{aligned}\frac{r_{P'}\sin\phi_{P'}-r_p\sin\phi_p}{r_{P'}\cos\phi_{P'}-r_p\cos\phi_p}&=-\tan(\theta-\phi_{P'}),\\ \theta&=\arctan\left(\frac{uv_{\rm M}-v_{\rm W}\sqrt{v_{\rm W}^2+u^2-v_{\rm M}^2}}{v_{\rm M}v_{\rm W}+u\sqrt{v_{\rm W}^2+u^2-v_{\rm M}^2}}\right).\end{aligned} \tag{20}$$

This tells that $\overline{PP'}$ is parallel to $(1,\theta-\phi_{P'})$; the angle between $\overline{PP'}$ and $\overline{P'O}$ is a constant θ independent of r_p,ϕ_p. Note that $\theta>0$ for $v_{\rm M}<v_{\rm W}$, and thereby every point P on mutant front with ϕ_p has its corresponding P' on sector boundary $\overset{\frown}{IB}$.

The next step toward identifying the front position at time T is to find all points P such that $T_{PP'I}=T$. Using the mapping between P and P' described above, we find P by first moving along sector boundary and then moving in a straight line parallel to $(1,\theta-\phi_{P'})$. By varying the time t' spent along the sector boundary while keeping the total time T fixed, we obtain a parametric expression for $P(T)=(x_p(T),y_p(T))$ in Cartesian coordinates:

$$\begin{aligned}x_p(T;t')&=(v_{\rm W}t'+r_0)\sin(\frac{u}{v_{\rm W}}\ln(\frac{r_0+v_{\rm W}t'}{r_0}))+v_{\rm M}(T-t')\sin(\frac{u}{v_{\rm W}}\ln(\frac{r_0+v_{\rm W}t'}{r_0})-\theta),\\ y_p(T;t')&=(v_{\rm W}t'+r_0)\cos(\frac{u}{v_{\rm W}}\ln(\frac{r_0+v_{\rm W}t'}{r_0}))+v_{\rm M}(T-t')\cos(\frac{u}{v_{\rm W}}\ln(\frac{r_0+v_{\rm W}t'}{r_0})-\theta).\end{aligned} \tag{21}$$

It is also possible to get a non-parametric, explicit expression by solving an equivalent partial differential equation using the method of characteristics:

$$\begin{aligned}\phi_p(t,r)&=\frac{u}{v_{\rm W}}\ln\left(1+\frac{v_{\rm W}t}{r_0}\right)+F\left(\frac{r}{r_0+v_{\rm W}t}\right)-F(1),\quad\text{where}\\ F(\rho)&=\frac{u}{2v_{\rm W}}\ln\left((\rho^2v_{\rm W}^2-v_{\rm M}^2)\frac{\sqrt{\rho^2-\frac{v_{\rm M}^2}{v_{\rm W}^2+u^2}}-\frac{uv_{\rm M}}{v_{\rm W}\sqrt{v_{\rm W}^2+u^2}}}{\sqrt{\rho^2-\frac{v_{\rm M}^2}{v_{\rm W}^2+u^2}}+\frac{uv_{\rm M}}{v_{\rm W}\sqrt{v_{\rm W}^2+u^2}}}\right)\\ &\quad+\arctan\left(\frac{\sqrt{v_{\rm W}^2+u^2}}{v_{\rm M}}\sqrt{\rho^2-\frac{v_{\rm M}^2}{v_{\rm W}^2+u^2}}\right).\end{aligned} \tag{22}$$

C.3. $v_{\rm M}>v_{\rm W}$. In this regime, $\theta<0$ and thereby some points P on the mutant front do not have a corresponding P' on the sector boundary. In other words, the straight path $\overline{IP}$ takes the shortest time. We find that, when P is near the top of the bulge, the minimal path is a straight line $\overline{IP}$ while, When P is further from the top, the minimal path is a straight line $\overline{P'P}$ followed by a curved path $\overset{\frown}{IP'}$ along the sector boundary.

Note that the straight path is tilted by a fixed angle θ from $\overline{OP'}$, pointing inwards to the center of the sector compared to the tangent line except when $v_{\rm M}=\sqrt{v_{\rm W}^2+u^2}$. In the latter case, $\theta=-\arctan\left(\sqrt{\frac{v_{\rm M}^2}{v_{\rm W}^2}-1}\right)$, and the straight path is tangent to the sector boundary, as described in (1).

The boundary between the two regions of the front lies angle $\phi_{\rm transition}$ way from the center. This angle is given by

$$\phi_{\rm transition}=\arctan\left(\frac{uv_{\rm M}-v_{\rm W}\sqrt{v_{\rm W}^2+u^2-v_{\rm M}^2}}{v_{\rm M}v_{\rm W}+u\sqrt{v_{\rm W}^2+u^2-v_{\rm M}^2}}\right). \tag{23}$$

Thus, the bulge is an arc of a circle near the center and is described by Eq. (21) near the sector boundary.

2. Dispersal without carrying capacity

In the main text, we considered two mechanistic models that produce all possible sector shapes. For both models, we assumed that the dispersal term has a factor of $(1 - n_{\mathrm{W}} - n_{\mathrm{M}})$ so that the dispersal ceases when population reaches the carrying capacity. Without the carrying capacity factor, any spatial patterns should eventually vanish because the populations continue to intermix behind the expanding front. Accordingly, sectors exist only in the transient timescale between expansion and diffusion. Nevertheless, the $(1 - n_{\mathrm{W}} - n_{\mathrm{M}})$ factor does not affect the ratios between three velocities v_{W}, v_{M} and u, and since these ratios determine the sector shape in geometric theory, we expect that the absence of the $(1 - n_{\mathrm{W}} - n_{\mathrm{M}})$ factor does not affect the sector shape observed in transient timescales. To verify this idea, we simulated a microscopic model without carrying capacity on diffusion:

$$\begin{aligned} \partial_t n_{\mathrm{W}} &= D\nabla^2 n_{\mathrm{W}} + r\left(1 - \alpha\frac{n_{\mathrm{M}}}{n_{\mathrm{W}} + n_{\mathrm{M}}}\right) n_{\mathrm{W}}(1 - n_{\mathrm{W}} - n_{\mathrm{M}}), \\ \partial_t n_{\mathrm{M}} &= D\nabla^2 n_{\mathrm{M}} + r\left(1 - s + \alpha\frac{n_{\mathrm{W}}}{n_{\mathrm{W}} + n_{\mathrm{M}}}\right) n_{\mathrm{M}}(1 - n_{\mathrm{W}} - n_{\mathrm{M}}). \end{aligned} \quad [24]$$

The simulation demonstrated that the sector shape was not affected by carrying capacity factor from dispersal (Fig. S12). The sector boundaries were blurred by the nonzero dispersal behind the front, but the overall shape of the sector remained the same.

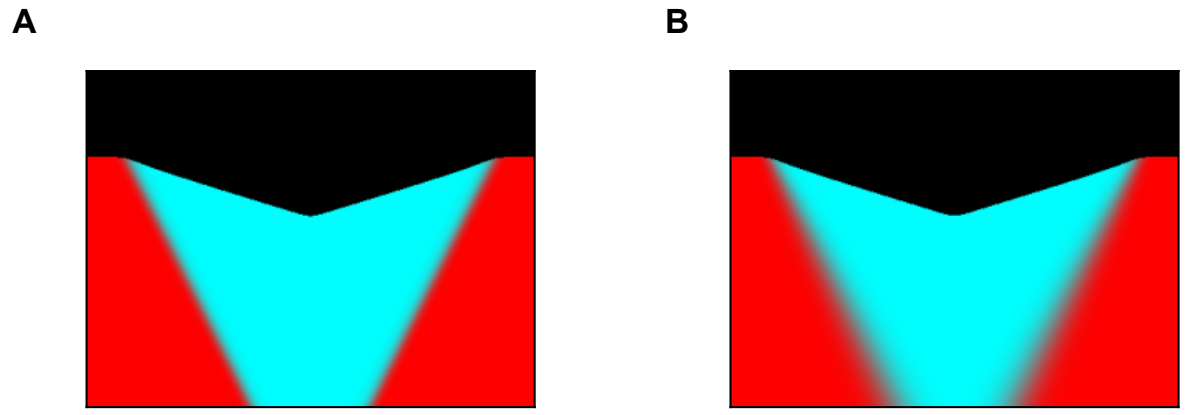

Fig. S12. Dented front in a model with density-independent dispersal. Formation of dented sectors in simulations with different models of dispersal. (A) The model from the main text Eq. 1. (B) A model with density-independent dispersal Eq. 24. Note the blurry sector boundaries due to continued intermixing after growth ceases behind the front.

3. Nonspatial limit for mechanistic models

In the main text, we considered two mechanistic models that produce all possible sector shapes. Here, we analyze these models in the nonspatial, i.e. well-mixed, limit, which describes local competition.

A. Cheater-cooperator model. The model reads

$$\begin{aligned}\partial_t n_{\rm W} &= \left(D\nabla^2 n_{\rm W} + r\left(1-\alpha\frac{n_{\rm M}}{n_{\rm W}+n_{\rm M}}\right)n_{\rm W}\right)(1-n_{\rm W}-n_{\rm M}),\\ \partial_t n_{\rm M} &= \left(D\nabla^2 n_{\rm M} + r\left(1-s+\alpha\frac{n_{\rm W}}{n_{\rm W}+n_{\rm M}}\right)n_{\rm M}\right)(1-n_{\rm W}-n_{\rm M}).\end{aligned} \quad [25]$$

In the well-mixed limit, the partial differential equations above reduce to a set of ordinary differential equations:

$$\begin{aligned}\frac{dn_{\rm W}}{dt} &= r\left(1-\alpha\frac{n_{\rm M}}{n_{\rm W}+n_{\rm M}}\right)n_{\rm W}(1-n_{\rm W}-n_{\rm M}),\\ \frac{dn_{\rm M}}{dt} &= r\left(1-s+\alpha\frac{n_{\rm W}}{n_{\rm W}+n_{\rm M}}\right)n_{\rm M}(1-n_{\rm W}-n_{\rm M}).\end{aligned} \quad [26]$$

We only consider $s<1$ and $-1<\alpha<1$ and assume that initial populations densities are positive and their sum is below the carrying capacity. With these assumptions, it is clear that the population densities remain positive for any $t\geq 0$ since $\frac{dn_{\rm W}}{dt}$ and $\frac{dn_{\rm M}}{dt}$ are positive. The monotonic increase of the population densities also ensures that $\lim_{t\to\infty} n_{\rm W}+n_{\rm M}=1$ because both time derivatives switch sign when $n_{\rm W}+n_{\rm M}$ exceeds unity. In fact, it follows directly from Eqs. (26) that any pair of positive $n_{\rm W}$ and $n_{\rm M}$ that sum up to one is a fixed point.

This line of fixed points is a direct consequence of our assumption that population dynamics are frozen behind the front. In a generic Lotka-Volterra system, the differences in the competitive abilities at high population densities would break this degeneracy and lead to the takeover by one of the types (stable coexistence is also possible) (1, 3). Microbial populations however grow only until the nutrients are exhausted, and the two types could, therefore, remain at an arbitrary ratio once the growth ceases.

Further insights into the behavior of Eq. (26) can be derived from its first integral (a conserved quantity), which we obtain by dividing the two equations:

$$\frac{dn_{\rm W}}{dn_{\rm M}} = \frac{\left(1-\alpha\frac{n_{\rm M}}{n_{\rm W}+n_{\rm M}}\right)n_{\rm W}}{\left(1-s+\alpha\frac{n_{\rm W}}{n_{\rm W}+n_{\rm M}}\right)n_{\rm M}}. \quad [27]$$

The equation above can be integrated after both sides are multiplied by $dn_{\rm M}(1-s+\alpha n_{\rm W}/(n_{\rm W}+n_{\rm M}))/n_{\rm W}$. This procedure yields the following conserved quantity:

$$C = \frac{(n_{\rm W}+n_{\rm M})^{\alpha} n_{\rm W}^{1-s}}{n_{\rm M}}, \quad [28]$$

which we can use to understand the temporal dynamics of the two types. It is convenient to recast Eq. (28) in terms of total population density $n=n_{\rm W}+n_{\rm M}$ and mutant frequency $f=n_{\rm M}/n$:

$$\frac{f}{(1-f)^{1-s}} = \frac{n^{\alpha-s}}{C}. \quad [29]$$

The left-hand side is a monotonically increasing function of f, and the right hand-side is a monotonic function of n, which is increasing for $\alpha>s$ and decreasing otherwise. Thus, f increases with n for $\alpha>s$ and decreases for $\alpha<s$. Since n is always increasing (assuming it is less than one initially), we conclude that the relative abundance of the mutant increases when $\alpha>s$ and decreases otherwise. Numerical simulations confirm this conclusion; see Fig. S13A.

In the spatial model, $u=\sqrt{\alpha-s}$, so the mutant can invade only when $s<\alpha$, which is consistent with the local well-mixed competition that we just described.

B. Growth-dispersal tradeoff model. The well-mixed limit for the growth-dispersal tradeoff model reads

$$\begin{aligned}\frac{n_{\rm W}}{dt} &= r n_{\rm W}(1-n_{\rm W}-n_{\rm M}),\\ \frac{n_{\rm M}}{dt} &= r(1+s)n_{\rm M}(1-n_{\rm W}-n_{\rm M}).\end{aligned} \quad [30]$$

The qualitative behavior of this system of equations is identical to that of the cheater-cooperator model. Any population below the carrying capacity with positive densities of the two types evolves to one of the neutral fixed points on $n_{\rm M}+n_{\rm W}=1$. The change of the mutant fraction can be determined from the following first integral

$$\frac{n_{\rm W}^{1+s}}{n_{\rm M}} = n^s\frac{(1-f)^{1+s}}{f} = C. \quad [31]$$

The analysis, identical to the one we just described, shows that the frequency of the mutant increases as long as $s>0$. This is consistent both with the expansion velocity $u=2\sqrt{Ds}$ and numerical simulations (Fig. S13).

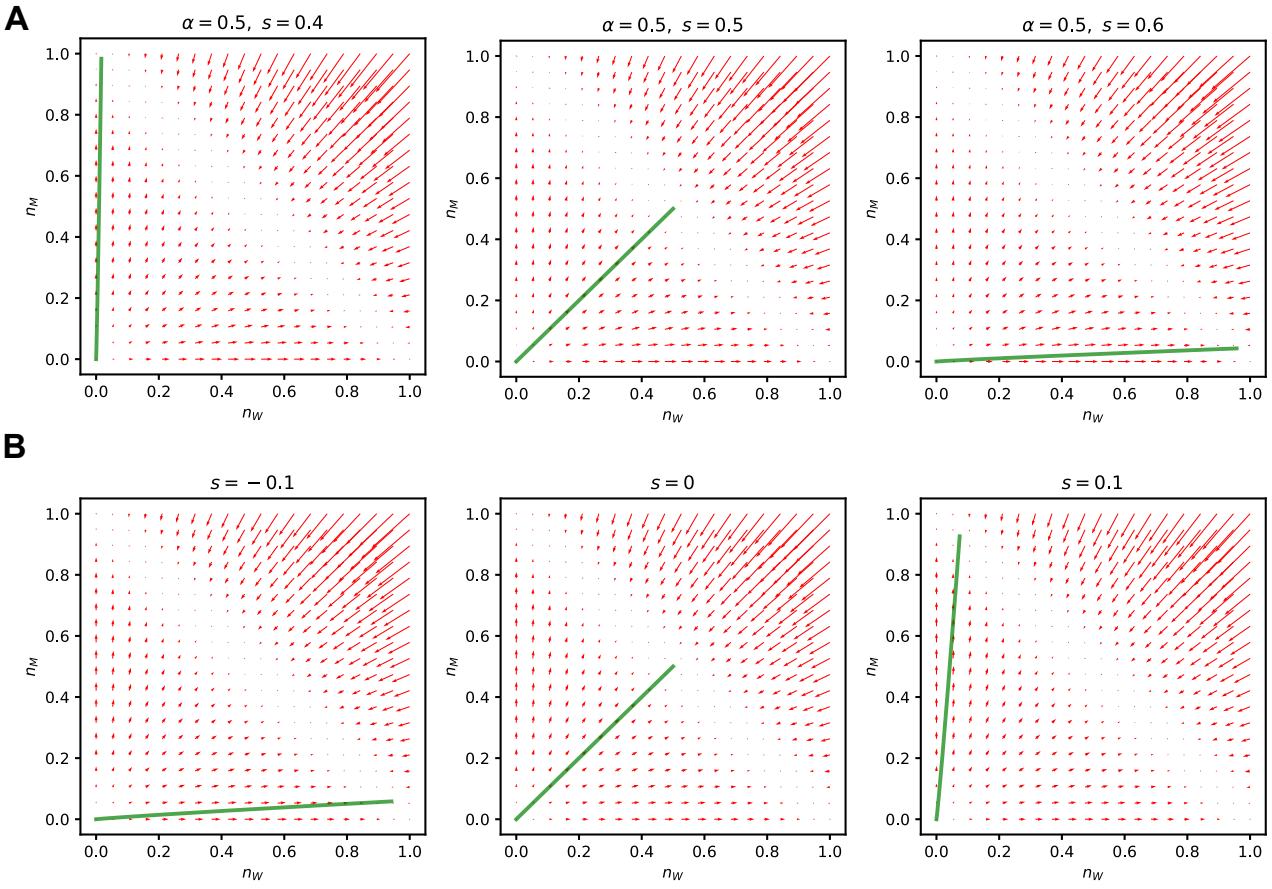

Fig. S13. Phase portraits of ODE dynamics. In each panel, red arrows represent $(dn_W/dt, dn_M/dt)$ and green curve shows the trajectory from small initial population $(n_W, n_M) = (10^{-12}, 10^{-12})$. (A) Phase portraits for cheater-cooperator interaction model. (B) Phase portraits for growth-dispersal tradeoff model.

References

1. KS Korolev, et al., Selective sweeps in growing microbial colonies. *Phys. Biol.* **9**, 026008 (2012).
2. M Born, E Wolf, *Principles of optics: electromagnetic theory of propagation, interference and diffraction of light*. (Elsevier), (2013).
3. JD Murray, *Mathematical Biology*. (Berlin: Springer), (2003).